Research Square

Preprints are preliminary reports that have not undergone peer review.
They should not be considered conclusive, used to inform clinical practice,
or referenced by the media as validated information.

The Assessment of Reservoir Sedimentation Using Optical and Microwave Sensors, and Water Level Data

Jogu Venkatesh
Jawaharlal Nehru Technological University, Hyderabad
Ravi Shankar Dwivedi
rsdwivedi51@gmail.com

Jawaharlal Nehru Technological University, Hyderabad

Article

Keywords: Live storage capacity, Interferometric Wide Swath (IW)mode, water year, trapezoidal formula

Posted Date: November 12th, 2026

DOI: https://doi.org/10.21203/rs.3.rs-11223837/v1

License: This work is licensed under a Creative Commons Attribution 4.0 International License.
Read Full License

Additional Declarations: No competing interests reported.

The Assessment of Reservoir Sedimentation Using Optical and Microwave Sensors, and Water Level Data

Jogu Venkatesh & Ravi Shankar Dwivedi

Centre for Spatial Information Technology

Jawaharlal Nehru Technological University

Hyderabad 500087, India

Abstract

Sedimentation of reservoirs is a perpetual threat to water security. A study was taken up to monitor the water storage capacities of the Nagarjuna Sagar reservoir in Telangana State, India, using cloud-free, pre-and post-monsoon multi-temporal Landsat-TM and OLI & TIRS data for the year 2001 to 2022, and Sentinel -1A and -1B Synthetic Aperture (SAR) data for the year 2022 to map spatial extent of water through digital analysis approach. The spatial extent of water, thus derived, was used in conjunction with *in situ* water elevation measurements to estimate the water storage capacities of the reservoir. The results show a good agreement between storage capacity derived from remotely sensed data and onsite storage capacity measurements with a RMSE, rRMSE and MAE values of 183.6Mm^3, 2.94% and 142,7Mm^3.A comparison of the storage capacities of the reservoir during the year 2022 and 2001, and 1968, the year of reservoir commissioning , reveals a drop in the storage capacity to the tune of 2,098.48Mm^3 accounting for 18.29% loss during the past 54years or an annual loss of 0.339% which is attributed to sedimentation. Ways to further improve the estimates of storage capacities of reservoirs using geospatial technologies are also highlighted.

Key Words: Live storage capacity, Interferometric Wide Swath (IW)mode, water year, trapezoidal formula.

1.0 Introduction

Reservoirs play a crucial role in water supply for hydroelectric power generation, irrigation, industrial and domestic purposes, and for recreation. All reservoirs across the world experience sedimentation of varying degrees. According to World Commission on Dams (2000) every year the siltation of reservoirs world over accounts for around 1% of the designed capacity. Churchill (1948) is pioneered with the prediction of reservoir sedimentation by linking the percentage of incoming sediment that passes through a reservoir with the sedimentation index. This index is defined as the ratio of the water's retention period to its mean flow velocity (Garg and Jothiprakash,2008). Using empirical curves, he related the loss in the reservoir capacity with basic hydrodynamic parameters. Sedimentation occurs due to settling down and gradual

accumulation of silt load in the reservoir due to reduction in the water velocity of the river when it reaches the reservoir resulting thereby in steady loss in its live storage capacity (Asthana and Khare, 2022). The loss in the live storage capacity results in diminishing the optimal functioning of the reservoir thereby posing a serious threat to its safety at the upstream as well as downstream of the dams (Wang and Kondolf,2014). Furthermore, variations in the rates of sedimentation have been attributed to terrain conditions, i.e. soils, land use/land cover (LU/LC), landslides and wildfires), catchment area and hydroclimate (Obialor et al., 2019; Sankey et al., 2017). Precise and timely information on water volume in a reservoir is of paramount importance for hydrological studies including definition of operating rules in simulation models (Yoon and Beighley, 2015), evaluation of the impact of the multi-reservoir systems on reservoir outflow (Vörösmarty et al., 1997; Hanasaki et al., 2006; Döll et al., 2009).

Conventionally, various methods, namely topographic differencing, acoustic sub-surface profiling , dynamic free-fall penetrometer measurements, and deep coring have been in vogue for assessment of reservoir sedimentation (Hilgert et al., 2024). Although detailed and precise these approaches are site-specific apart from being time and cost-prohibitive. By virtue of characteristic spectral response pattern water optical sensor data have been extensively used for delineation of water bodies. However, persistent cloud cover during rainy season precludes delineation of water bodies using optical sensor data. Microwave sensors data with 'see-through cloud" capability are, therefore, used for surface water mapping during rainy season. With regard to surface water elevation, data from altimeters operating in optical as well as microwave region of the electromagnetic spectrum are employed. In fact, spatial extent of water in a reservoir at a given point of time physically outlines the topographic contour for that water elevation. Storage capacity is estimated by aggregating different contours between them (Codjia et al, 2025).

2.0 The Role of Remote Sensing

Conventionally, various methods, namely topographic differencing, sub-bottom profiling, dynamic free-fall penetrometer measurements, and long sediment coring have been in vogue for reservoir sedimentation (Hilgert et al., 2024). These methods are point-specific apart from being time and cost prohibitive. Remotely sensed data, in general, and orbital sensor data, in particular, offer immense potential in estimation of spatial extent of water in a reservoir. Microwave sensors especially synthetic aperture radar (SAR) data provides information on

water spread area even during rainy season characterized by the presence of persistence cloud cover.

Water-spread area, thus derived from remotely sensed data, is used to determine the volume of water in a reservoir in conjunction with water level data available with the reservoir authorities or derived from satellite altimeter data (Patra, 2001). Several studies have been carried out on the applications of orbital sensors data in estimation of the storage capacity of a reservoir (Vibulsresth,1988; Goel et al.,2002; Abileah and Vignudelli 2011; Gourgouletis et al.,2022; Shen et al.,2022). While working in the lake Nasser in southern Egypt and part of Sudan Abileah and Vignudelli (2011) estimated the volume of water in the lake using spatial extent of water derived from Landsat-TM data and water level(elevation) from radar altimeter data.

We have used Landsat-8 OLI&TIRS and Sentinel-1A and-1B-SAR data for estimation of water spread area and water level data from on-site measurements to investigate the temporal patterns of storage capacities and assess the sedimentation of the Nagarjuna Sagar reservoir situated in a semi-arid region of peninsular India.

3.0 Test Site

Nagarjuna Sagar dam (16°34′32″N and 79°18′42″E) has been built during the period 1955 and 1967across the Krishna river at the Nandikonda village in Pedavoora *mandal* of Nalgonda district, Telangana State, India (Central Water Commission, 2021; https://irrigation.telangana.gov.in/img/projectspdf/nsp.pdf) (Figure-1). Built in 1968 with a gross storage capacity of 11.472 billion cubic metres (https://www.krmb.gov.in/html/project39.html) the reservoir consists of a 124.7 metres high masonry dam and the two canal systems i.e.. Right Bank Canal and Left Bank Canal and their distributary systems with a command area of 8.95 lakh ha. In addition it provides water for hydro-electric power generation up to 960 MW(Central Water Commission, 2021). The catchment receives a mean annual precipitation of 772mm., of which an estimated 71% is received during the month of June to September (jntuhist.ac.in).

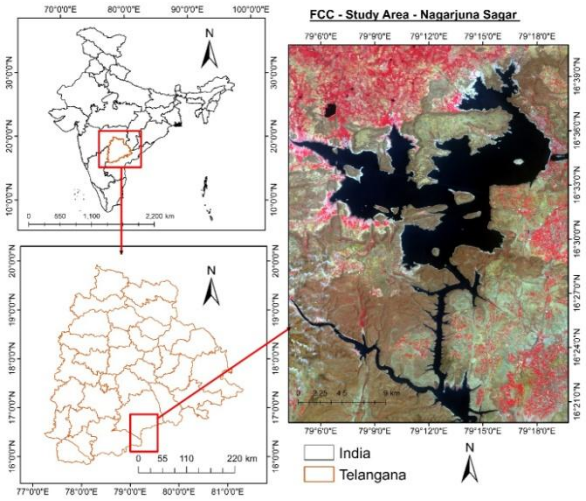


Figure-1: Location map of the test site.

3.0 The Approach

3.1Database

3.1.1Optical Sensor Data

Selection of the data for appropriate period plays a very crucial role in estimation of reservoir capacity using remotely sensed data. Although logically for assessment of siltation of reservoirs time-series monthly data for entire water year need to be analysed, due to cloud infestation over the test site during rainy season(June to September only a few months cloud-free remotely sensed data could be used. The term "water year" refers to a 12-month period commencing from October 1 of a particular year through September 30, of the subsequent year. Generally, it is designated by the calendar year in which it ends (https://water.usgs.gov/vizlab/water-availability/glossary).In India, the end of monsoon (October–November) is the period when most of the reservoirs generally reach the maximum water level followed by a gradual decrease in water level during succeeding period of the year until the arrival of the next rainy season(June–July). As mentioned earlier, since the presence of cloud cover during monsoon season precludes capturing water features by optical sensor data, the Landsat-TM/OLI/TIRS data (https://earthexplorer.usgs.gov) collected during pre- and -post-monsoon period for the years 2001, 2002, 2016, 2017, 2018, 2021 and were used for reservoir capacity estimation (Table-1).

Table-1 List of Landsat-TM/OLI&TIRS data used.

S.No.	Date of pass*	Water level(m)	S.No.	Date of pass*	Water level(m)
1	23-10-2001	175.32	16	19-05-2017	153.59
2	12-12-2001	166.68	17	14-11-2018	171.30
3	24-12-2001	164.74	18	03-03-2018	159.22
4	25-02-2002	157.03	19	22-05-2018	156.12
5	14-09-2002	156.94	20	21-10-2021	179.71
6	11-05-2002	154.72	21	08-12-2021	178.90
7	27-11-2002	153.19	22	14-03-2021	166.66
8	22-12-2002	152.28	23	13-04-2021	165.44
11	08-11-2016	163.03	24	30-05-2021	162.46
12	10-02-2016	155.17	25	09-01, 2022	177.06
13	16-05-2016	154.72	26	10-02- 2022	176.17
14	27-11-2017	172.79	27	30-03-2022	167.67
15	28-02-2017	156.11	28	17-05-2022	163.92

*The dates of Landsat data used are arranged in descending order of water level in the reservoir in a particular calendar year.

3.1.2 Microwave Sensor Data

In tropical region owing to the presence of cloud infestation during monsoon season (June to September) cloud-free optical sensor data is, generally, not available which precludes the estimation of the capacity of a reservoir for entire water year. Data from microwave sensors with cloud-penetration capability offer immense potential in the investigation of any phenomenon or process throughout the year in cloud-infested regions. We have used time-series Sentinel-1 SAR data of the reservoir for water year 2022 (one image per month) collected in the Interferometric Wide swath (IW) mode (Table-2) for storage capacity estimation(https://dataspace.copernicus.eu/data-collections/copernicus-sentinel-missions/sentinel-1).

.

Table-2 Details of Sentinel-1 SAR data used.

S. No.	Date of satellite overpass	S. No.	Date of satellite overpass
1	13-06-2021	7	15-12-2021
2	12-07-2021	8	08-01-2022
3	17-08-2021	9	13-02-2022
4	10-09-2021	10	09-03-2022
5	16-10-2021	11	09-04-2022
6	09-11-2021	12	08-05-2022

As part of European Space Agency's Copernicus programme, the Sentinel-1 constellation (S-1 A & S-1B, launched on April 3, 2014, and April 22, 2016, respectively) uses two radar satellites in the same orbital plane but 180° apart, enabling a combined 6-day revisit time for frequent, dual-polarized (VV&VH) imaging of the Earth, crucial for applications like environmental monitoring, sea ice tracking, and disaster management (https://sentiwiki.copernicus.eu/web/s1-mission) (Table-3).

Table-3 Salient features of Sentinel-1 SAR sensor.

Central frequency: 5.405 GHz (wavelength of ~5.54cm)

Band width : 0-100 MHz (programmable)

Polarization: Dual (VV and VH)

Incidence angle: 20°- 46°

Look direction: right

Pulse width: 5-100μs (programmable)

Data quantization: 10 bit

Spatial resolution- 10m

Offering four acquisition modes: Strip map (SM), Interferometric Wide swath (IW), Extra-Wide swath (EW), and Wave (WV), the SAR operates at C-band (5.407 GHz)(Torres et al., 2012). The IW mode uses Terrain Observation with Progressive Scans SAR (TOPSAR) technique to offer a wide 250 km coverage with moderate 5m x 20m resolution, capturing three sub-swaths by electronically steering the beam in range and azimuth to eliminate scalloping,

ensuring consistent image quality and enabling high-quality Interferometric SAR (InSAR) analysis through overlapping Doppler spectra (https://sentiwiki.copernicus.eu/web/s1-mission).

3.1.3Ancillary Data

The ancillary data includes *in situ* measurements on daily water level in the reservoir in feet, storage capacity in TMC, outflow in cusecs, evaporation losses, and river inflow from June 1985 to September 2022 made by the Nagarjuna Sagar Reservoir Authority, Irrigation and Command Area Development, Government of Telangana, India. In addition, rainfall data from the India Meteorological Department, Government of India was also used. A sample of part of the data is appended as Table-4.

Table-4 A sample of the part of on-site reservoir data.

S. No.	Date	Reservoir inflow (cusecs)	Reservoir level (feet)	Gross storage (TMC*)
1	1-Aug-21	414526	579.20	280.6992
2	2-Aug-21	421286	587.20	305.6242
3	3-Aug-21	344078	587.00	305.5050
4	4-Aug-21	133554	588.20	306.6922
5	5-Aug-21	129246	589.70	311.1486
6	6-Aug-21	184961	588.80	308.4658
7	7-Aug-21	113437	589.70	311.1486
8	8-Aug-21	66667	590.00	312.0450
9	9-Aug-21	65098	589.90	311.7462
10	10-Aug-21	73879	589.60	310.8498
11	11-Aug-21	91906	589.70	311.1486
12	12-Aug-21	91783	589.50	310.5510
13	13-Aug-21	62574	589.70	311.1486
14	14-Aug-21	59695	589.80	311.4474
15	15-Aug-21	60644	589.60	310.8498

*TMC = Thousand Million Cubic feet, One TMC =~ 28.3 billion litters of water.

Source: Nagarjun Sagar Reservoir Authority, Government of Telangana, India.

3.2 The Approach

3.2.1 Analysis of Landsat-8 OLI &TIRS Data

To begin with, radiometric normalization of multi-temporal Landsat-TM/ OLI& TIRS images was carried out to account for variations in illumination and atmospheric conditions using pseudo-invariant features(PIFs) (Schott et al., 1988)(Figure-2). PIFs are man-made features such as concrete, asphalt, and rooftops with reasonably constant reflectance over time.

Differences in the reflectance of PIFs between two time periods is surmised to be associated with the variations in atmospheric conditions, and are a linear function. These differences are corrected statistically during radiometric normalization.

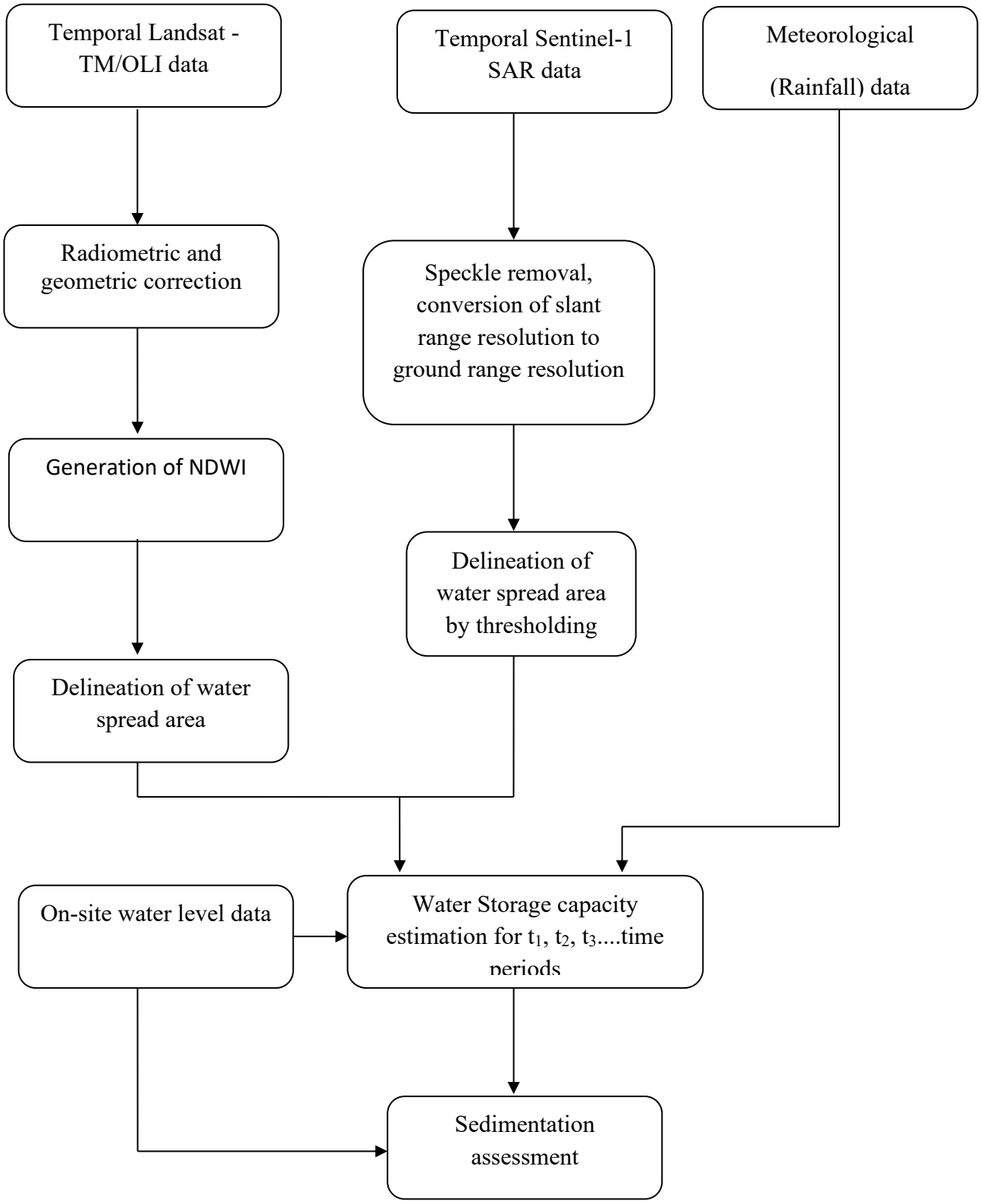


Figure-2 Schematic diagram of the approach.

The digital classification methods commonly used for water classification from optical sensor data could be grouped into 4 categories (Ji et al., 2009): "(i) thematic classification, (ii) linear unmixing, (iii) thresholding and (iv) the use of spectral indices (McFeeters, 1996; Xu, 2006)". Amongst these methods, two-band spectral water indices have been generally used when the purpose is to delineate only water bodies. Included in the spectral indices are: Normalized Difference Water Index (NDWI) (McFeeters,1996) and its variant, Modified NDWI (mNDWI) (Xu, 2006), the High Resolution Water Index (Yao et al., 2015), the 2015 Water Index (WI2015) (Fisher et al., 2016), and two Automatic Water Extraction Indices (AWEInsh and AWEIsh) (Feyisa et al., 2014). We have used NDWI, a two-band spectral index, derived from Landsat-8 OLI datasets to map water spread area using the following formula (McFeeters,1996):

$$NDWI = \frac{\rho\lambda_1 - \rho\lambda_2}{\rho\lambda_1 + \rho\lambda_2} \quad \text{-- (1)}$$

where $\rho\lambda_1$ is the spectral reflectance in green spectral band , and $\rho\lambda_2$ is the spectral reflectance in near IR spectral band. In the output image of NDWI water bodies appear as white whereas vegetation and other terrain features are seen as black.

Although several spectral indices like NDWI and MNDWI, Automated Water Extraction Index, Water Ratio Index (WRI) have been in vogue for extraction water spread area, defining universally applicable optimum threshold for these indices has been a challenging task because of variations in terrain and atmospheric conditions. The double-window flexible pace search (DFPS) method developed by Chen et al.(2003) has been found to be more effective in delineation of pure water pixel (Choudhary and Ghosh,2022; Piyoosh and Ghosh, 2017).

3.2.2 Analysis of Sentinel-1 SAR Data

To begin with , the Level-1 Ground Range Detected (GRD) product Interferometric Wide (IW) swath data, was downloaded from the Copernicus Open Access Hub (https://scihub.copernicus.eu/dhus), an open platform for Sentinel data. Images were subsequently pre-processed in the Sentinel Application Platform (SNAP) with the Sentinel-1 Toolbox(S1TBX) for orbital correction, thermal noise removal, calibration, speckle filtering; range doppler terrain correction, and conversion of DN values backscattering coefficient

(sigma naught-σ^0) values in dB. It was followed by creation of multi-layer stack of time-series SAR images. Lastly, threshold approach was employed to delineate water pixels (Otsu, 1979)

3.3 Water Storage Capacity Estimation

The assessment of sedimentation using remotely sensed data is based on the premise that the deposition of sediments or silt in the reservoir will result in the reduction of water spread area at a given water level or elevation and will eventually lead to loss in the storage capacity of the reservoir (Goel et al., 2002).The water storage capacity of the reservoir is estimated by calculating the volume of water at two water levels or elevations assuming the volume of water stored at two elevations as trapezoid, The storage capacity is estimated using the trapezoidal or the prismoidal or the Simpson formula (Patra, 2001). Amongst these approaches, the use of the trapezoidal formula has been very common for assessment of the storage capacity of the reservoirs (Goel and Jain 1996; Rathore, 2006).For estimation of reservoir capacity the water-spread area we have used Landsat-TM OLI data/ Sentinel-1SAR data in conjunction with corresponding reservoir water-level measurements made on-site by the Nagarjuna Sagar dam authorities, Government of Telangana as follows:

$$\Delta V = \Delta H/3\ [(A_1 + A_2 + \sqrt{(A_1 * A_2)}] \quad .....(1)$$

where V is the volume between two consecutive water elevations. A_1 and A_2 are the water-spread area at the reservoir water elevation 1 and 2, respectively and ΔH is the difference between these two water levels.

Eventually volume of water at all consecutive water levels , thus estimated, were summed up to get the storage capacity of the reservoir.

4.0 Results and Discussion

The results of the study are described in two sections, namely storage capacity estimation and assessment of siltation.

4.1Storage Capacity Estimation

As mentioned in Section-3,3 reduction in the live capacity of the reservoirs is primarily associated with the sedimentation or siltation. Reservoir sedimentation has always been a challenge for dam authorities. Annually 0.5–1% of global storage volume is estimated to be lost to sedimentation (Basson, 2009). Conventional methods for assessing reservoir

sedimentation, which involves the gradual accumulation of sediment, include inflow-outflow methods, capacity surveys, integrated bathymetric surveys and remote sensing techniques. For further details on reservoir sedimentation refer (e.g., Rausch and Heinemann,1968). The amount of capacity lost to sedimentation could be subsequently evaluated from the comparison of the original and revised elevation–capacity curves (Vishwakarma et al. 2015; Merina et al. 2016). Although *on-site* observations on various parameters have been available for the period 1985 to 2022 due to non-availability of *on-site* sedimentation data required for validation the conventional approach for assessment of sedimentation could not be applied.

In essence the approach involves assessment of the long-term changes in spatial extent of surface water in the reservoir using time-series orbital sensors data and the information on water level(elevation) from on-site measurements. For quantification of the capacity of a reservoir, the water-spread area at different water levels of the reservoir is estimated (Morris and Fan 1998, Peng 2006). Using trapezoidal formula incremental/ segmental water storage capacity for a water column between two water levels have been estimated. In order to study sedimentation multi-temporal Sentinel-1A SAR data have been used. Incremental water volume values, thus obtained, were aggregated to estimate cumulative storage capacity of the reservoir. Ideally, variations in long-term reservoir capacity values are required for assessment of sedimentation. Although Landsat-TM/ OLI/TIRS data for the period 2001, 2002,2016, 2017 , 2018, 2021 and 2022 were used for estimation of water spread area, owing to cloud cover/other data quality issues complete dataset for any water year could not be analysed. In order to obviate the cloud cover limitation Sentinel-1A and 1B SAR data for the water year 2021-2022 was used for estimation of storage capacity of the reservoir.

4.1.1 Landsat-8OLI&TIRS Data

Selection of the data for appropriate period plays a very important role the estimation reservoir capacity using remotely sensed data. In India, reservoirs achieve their full storage capacity after withdrawal of monsoon(rainy season) during October–November. Thereafter there is a gradual decrease in water volume during subsequent period of the year until the onset of the next monsoon (June –July). The changes in water-spread could be accurately estimated by analysing the water spread area of the reservoir at different water levels over a period of time using digital chrono-sequential satellite data (Morris and Fan 1998; Smith and Pavelsky 2009). As mentioned in Section 3.3 , water spread area derived from Landsat-TM / OLI and data using NDWI was used in conjunction with and water level values available from on-site

measurements for estimation of the storage capacity of the reservoir. Moreover, water spread was derived from cloud-free good quality Landsat-TM/OLI&TIRS data for the year2001,2002,2016, 2017, 2018, 2021 and 2022 (Table-1). A typical example of water spread maps developed from Landsat8-OLI and TIRS data for the water year 2022 is appended as Figure-3.

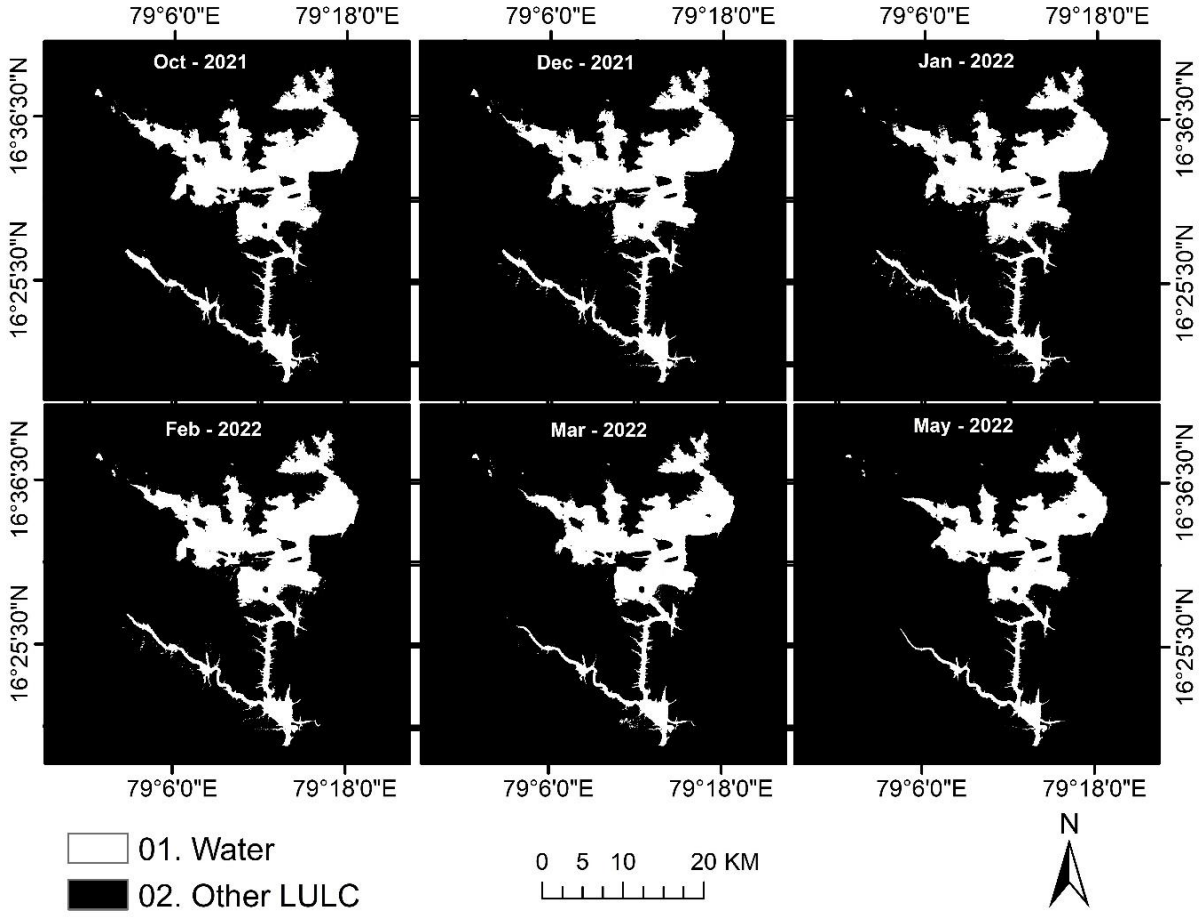


Figure-3 The dynamics of water spread area (white colour) in the reservoir. Non-water features like crops, scrubs, forests and rock outcrops are seen as dark colour (Adopted from Venkatesh et al.,2023).

In this figure, maps showing water spread area are arranged according to calendar months of a water year 2022 covering the period October 2021 to September 2022. The estimated water spread area for the period October2021 to May2022 along with other periods (2001 to 2018) is appended as Table-5. A critical analysis of water spread areas for water year2022 (calendar year 2021-2022) (Figure-3) reveals a progressive shrinkage in the water spread area of the reservoir with the approaching dry season which is corroborated well by the corresponding variations in the water spread area figures (Table-5). While delineating water spread area of the Nagarjuna Sagar reservoir from Indian Remote Sensing Satellite(IRS-1-C and-1D data Jeyakanthan and Sanjeevi (2013) used a sub-pixel or linear mixture model (LMM) approach

to avoid mixing of soil and vegetation pixels with the water pixels. The water spread area, thus derived, has been used to estimate the capacity of the reservoir in conjunction with *on-site* water level measurements.

Table-5 Reservoir capacity as derived from Landsat-TM/OLI data.

S.No.	Date of pass	Water level(m)	Water spread area (Mm^2)	Segmental capacity (Mm^3)	Cumulative capacity (Mm^3)
2001					
1	23-10-2001	175.32	238.55	1908.67	10,061.33
2	12-12-2001	166.68	203.73	384.68	8,152.66
3	24-12-2001	164.74	192.89	-	7,767.98
2002					
4	25-02-2002	157.03	173.75	15.33	6,019.17
5	14-09-2002	156.94	166.93	366.74	6,003.84
6	11-05-2002	154.72	163.47	244.90	5,637.1
7	27-11-2002	153.19	156.69	141.27	5,392.2
8	22-12-2002	152.28	153.79	-	5,250.93
2016					
11	08-11-2016	163.03	264,86	1735.85	5,435.66
12	10-02-2016	155.17	179.59	72.39	3,699.81
13	16-05-2016	154.72	142.86	-	3,627.42
2017					
14	27-11-2017	172.79	322.46	4074.70	7,912.19
15	28-02-2017	156.11	173.72	396.52	3,837.49
16	19-05-2017	153.59	141.53	-	3,440.97
2018					
17	14-11-2018	171.30	282.12	2758.02	7,096.22
18	03-03-2018	159.22	179.18	504.02	4,338.2
19	22-05-2018	156.12	147.56	-	3,834.18
2021					
20	21-10-2021	179.71	262.07	209.88	8,653.21
21	08-12-2021	178.90	256.17	2822.78	8,443.33
22	14-03-2021	166.66	168.14	199.41	5,620.55
23	13-04-2021	165.44	159.35	482.17	5,421.14
24	30-05-2021	162.46	164.38	-	4,938.97
2022					
25	09-01-2022	177.06	248.04	162.73	8,173.85
26	10-02- 2022	176.17	251.80	2012.38	8,011.12
27	30-03-2022	167.67	222.56	796.11	5,998.74
28	17-05-2022	163.92	202.18	-	5,202.63
	Minimum Draw Down Level (MDDL)	155.54			3,727.54

To monitor the spatial extent of surface water dynamics, change detection is usually resorted to. Two types of change detection methods are in vogue: the first method involves

classification of multi-temporal images followed by identification of areas with expansion or shrinking of water bodies. The second method encompasses direct comparison of images acquired at different point of time, and subsequent classification of comparison results into different change status. Included in the second method are image differencing (Wang, 2004; Wang et al., 2002), principal component analysis (Rokni et al., 2014; Gianinetto et al., 2006), and change vector analysis (Huang et al., 2016; Landmann et al., 2013). For further details on monitoring surface water using optical sensor data refer (e.g., Wang and Xie. 2018; Huang et al., 2018; Jawak et al., 2015).

As evident from Table-5, during the water year 2022 (October 2021 to September 2022),there has been incremental shrinkage in water spread areas from retreating monsoon in October 2021 (262.07Mm^2) to extremely hot and dry season during April13, 2021(159.35Mm^2). Further, the cumulative storage capacity of the reservoir ranges between 5202.63Mm^3 on May17,2022 to 8,653.21Mm^3on October 21, 2021.As mentioned in Section3.1.1, in addition to these Landsat-OLI/TIRS images some more Landsat-8TM/OLI images were analysed to delineate water spread area following similar approach that was followed for analysis of these six images. Information on water level, water spread area and gross storage capacities, thus derived, is given in Table-5.

4.2.2 Sentinel-1SAR Data

The detection of water features from microwave sensors data is based on specular reflection from water. A flat and smooth water surface behaves like a mirror and reflects the incident microwave radiation away from the sensor which results in low backscatter, and makes water bodies to appear as very dark regions in the SAR image (Guo et al., 2022) in the backdrop of adjoining land surfaces. However, return signals may be attenuated by wave action on the water surface (Sheffield et al., 2018). In order to delineate surface water bodies within North Carolina and South Carolina (Wang,2004) used a single decision tree classifier on two sets of Japanese Earth Resources Satellite-1(JERS-1) SAR data and achieved an overall classification accuracy of nearly 90%.(Wang, 2004). Pham-Duc et al.(2017) developed a method for detection and monitoring surface water bodies in the Cambodia and the Vietnamese Mekong Delta from Sentinel-1SAR data collected on Decemebr17,2015. The method is based on artificial neural network(ANN) network classifier that was trained with Landsat-8 OLI&TIRS data. The results show a spatial correlation of 0.90 as compared to Landsat-8OLI&TIRS data. Microwave radiometers detect the lower brightness temperature of the water, but suffer from

low spatial resolution that makes them less useful in observing smaller or complex water bodies and inundation (Sheffield et al., 2018).

As mentioned in Section-3.3.1 owing to the presence of cloud cover Landsat-TM and OLI&TIRS data for April, June to September and November could not be used for analysis. Taking advantage of cloud-penetration capability Sentinel-1A SAR data for the period June2021 to May 2022 was used for extraction of water spread area of the reservoir. As evedent from Figure-4 water in the reservoir appear as dark gray features owing to its smooth surface contributing to specular reflection. Also refers to as mirror-like reflection, specular reflection is the reflection of electromagnetic radiation from a smooth surface where the angle of reflection equals the angle of incidence. The Sentinel-1A&-1B SAR data and water spread areas derived there from are appended as Figure-5and -6, respectively and the area statistics in Table-6. As evident from Table-6, water spread area ranges from 215.45 Mm^2 in the month of July (12-07-2021) to 269.45 Mm^2 in October month (16-10-2021).

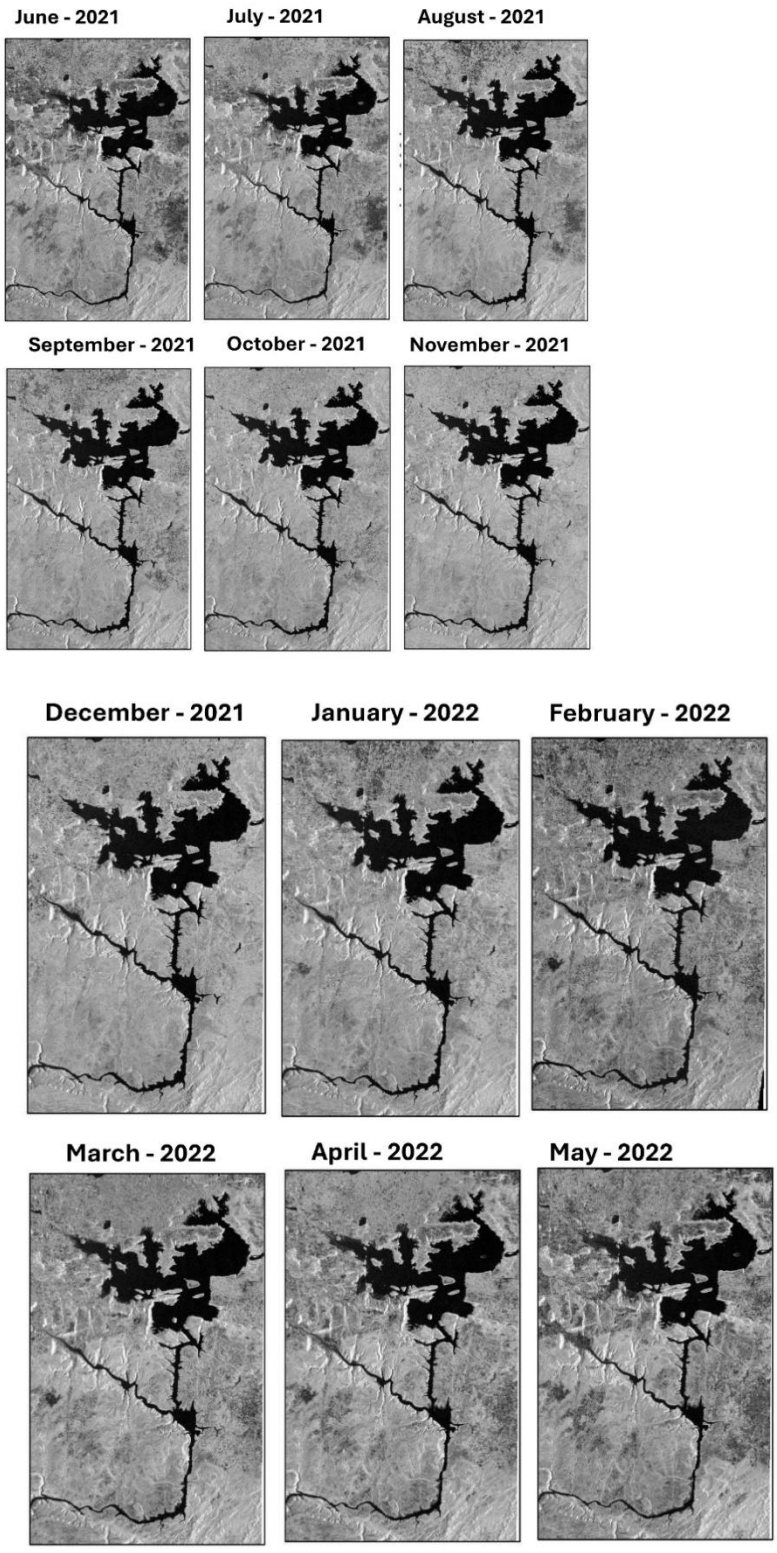


Figure-4: Multi-temporal (June2021 to May2022) Sentinel-1SAR data of the reservoir.

Table-6: Storage capacity of the reservoir as derived from Sentinel-1 SAR data.

S. No.	Date of satellite overpass	Water levels(m)	Water spread area (Mm^2)	Segmental water volume (Mm^3)	Cumulative water volume (Mm^3)
1	16-10-2021	179.77	269.45	8.07	9,373.52
2	09-11-2021	179.74	268.72	16.14	9,365.45
3	17-08-2021	179.80	269.39	218.08	9,349.31
4	10-09-2021	178.98	269.00	99.09	9,131.23
5	15-12-2021	178.61	268.08	531.55	9,032.14
6	13-02-2022	176.60	260.85	104.65	8,500.59
7	08-01-2022	176.20	263.75	960.63	8,395.94
8	09-03-2022	172.49	254.42	1618.55	7,435.31
9	09-04-2022	165.99	245.16	460.76	5,816.76
10	08-05-2022	164.10	242.42	391.16	5,356.00
11	13-06-2021	162.43	226.70	236.08	4,964.84
12	12-07-2021	161.36	215.45	-	4,728.16

A close look at Table-6 reveals a large variation in the cumulative storage capacities ranging from 9,373.52 Mm^3 in October (16-10-2021) to 4,728.16Mm^3 in July (12-07-2022)(Figure-5 and-6).

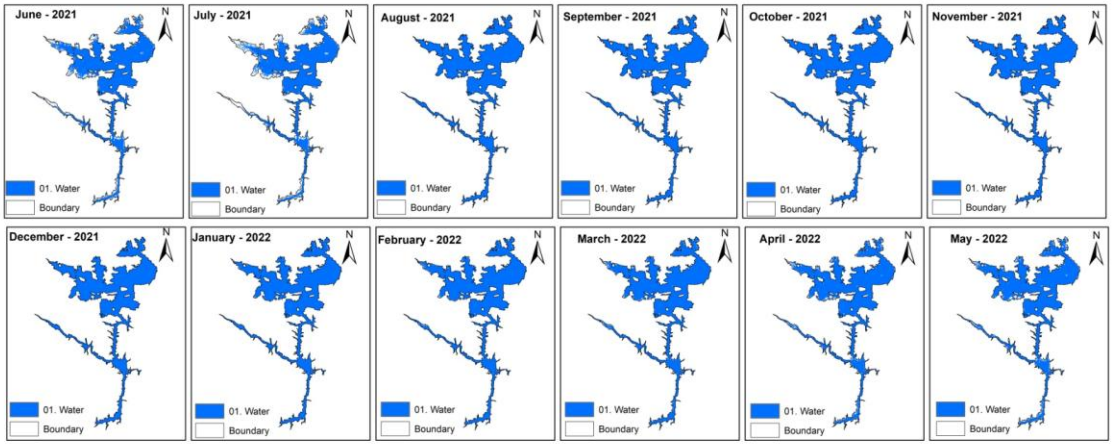


Figure-5 Monthly water spread areas from June 2021 and May 2022 as derived from Sentinel-1 SAR data.

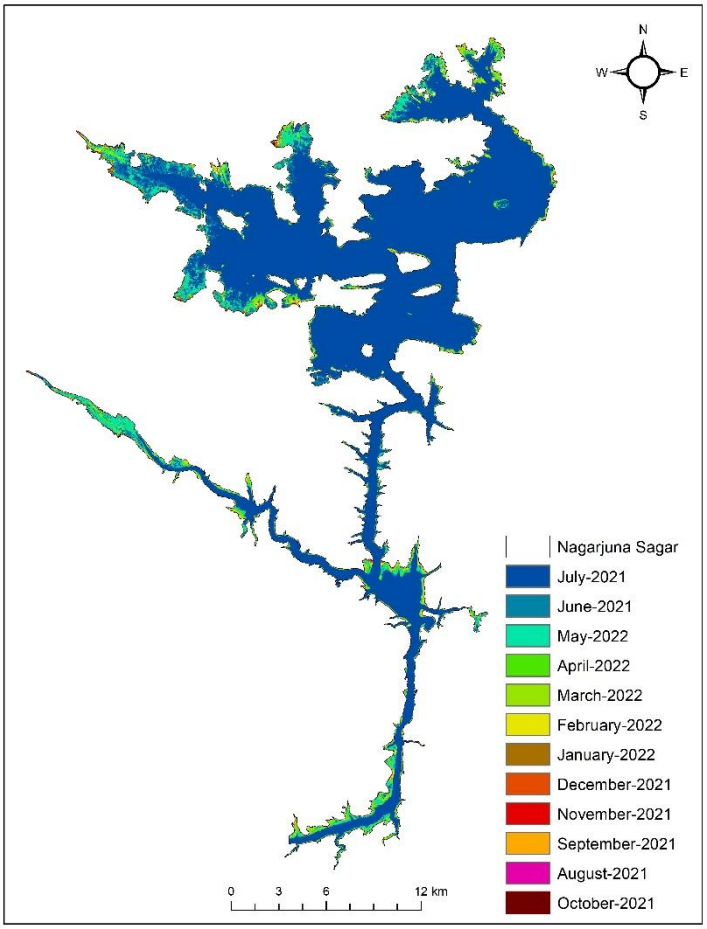


Figure-6: Intra-annual variations in water spread area as derived from Sentinel-1SAR data.

4.2.2.1 Water Level-Storage Capacity Relationship

An attempt was also made to establish the relationship between water level and cumulative storage capacity of the reservoir. Cumulative storage capacity values for12 days-one each for every month for 12 months as derived from Sentinel1A/1B SAR data against corresponding water levels of the reservoir recorded on-site (Figure-7). A best-fit polynomial equation of second order as given below has been derived.

$Y = 2.428x^2-579.23x+35041$ …(2)

$R^2 = 0.9996$

where, x is elevation in meters and y is cumulative gross storage capacity in Mm^3.

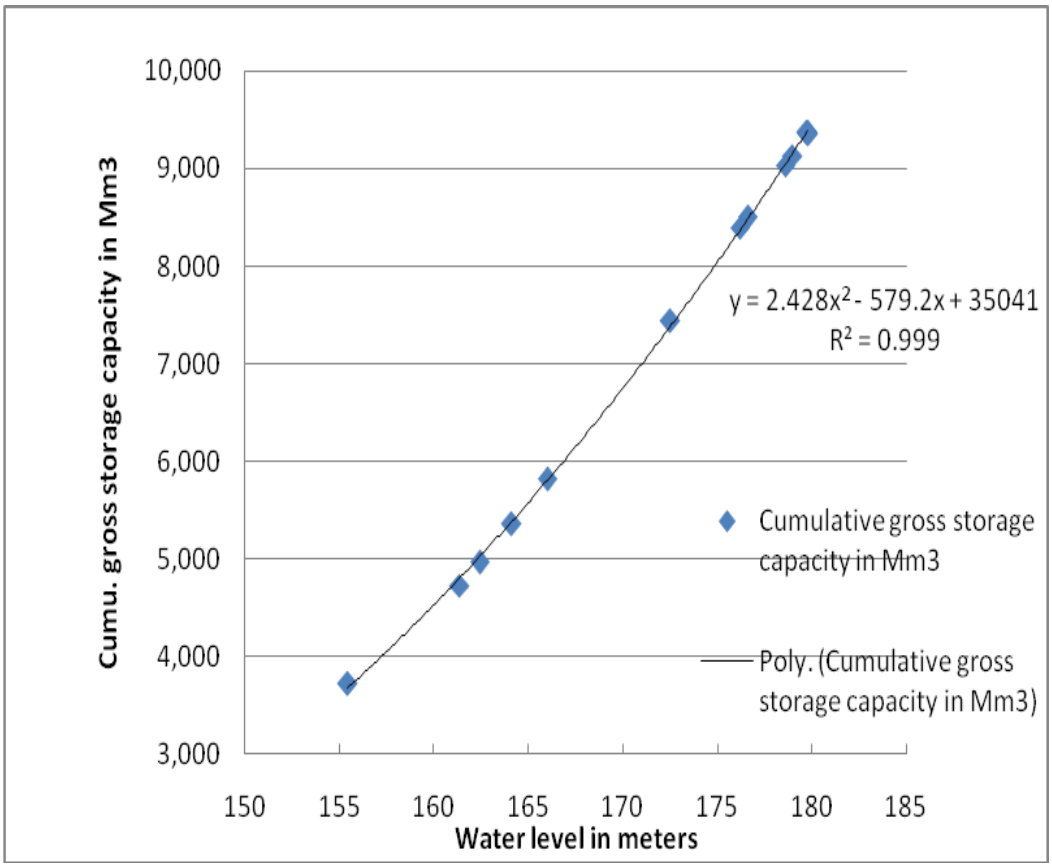


Figure-7: Water level-cumulative storage capacity as derived from Sentinel-1 SAR data.

A close look at the Figure-6 reveals a linear relationship between water level and cumulative storage capacity.

4.2.3 Validation of Storage Capacity

For assessment of robustness of the approach for estimation of the cumulative storage capacity of the reservoir, a comparison was made between the storage capacity values, 40 in number,

derived from Landsat-TM/OLI and Sentinel-1 SAR data and those recorded on-site by the Nagarjuna Sagar Authority**.** As evident from Figure-8, there is a good agreement between remotely sensed derived storage capacity and those recorded on-site with a R^2 value of 0.972 and RMSE and mean absolute error (MAE) values of 183,6 $Mm^3$and 142.7Mm^3, respectively. Further, the relative root mean square error rRMSE works out to be 2.94%.These results vividly demonstrate the potential of remotely sensed data in the estimation of storage capacity of the reservoir.

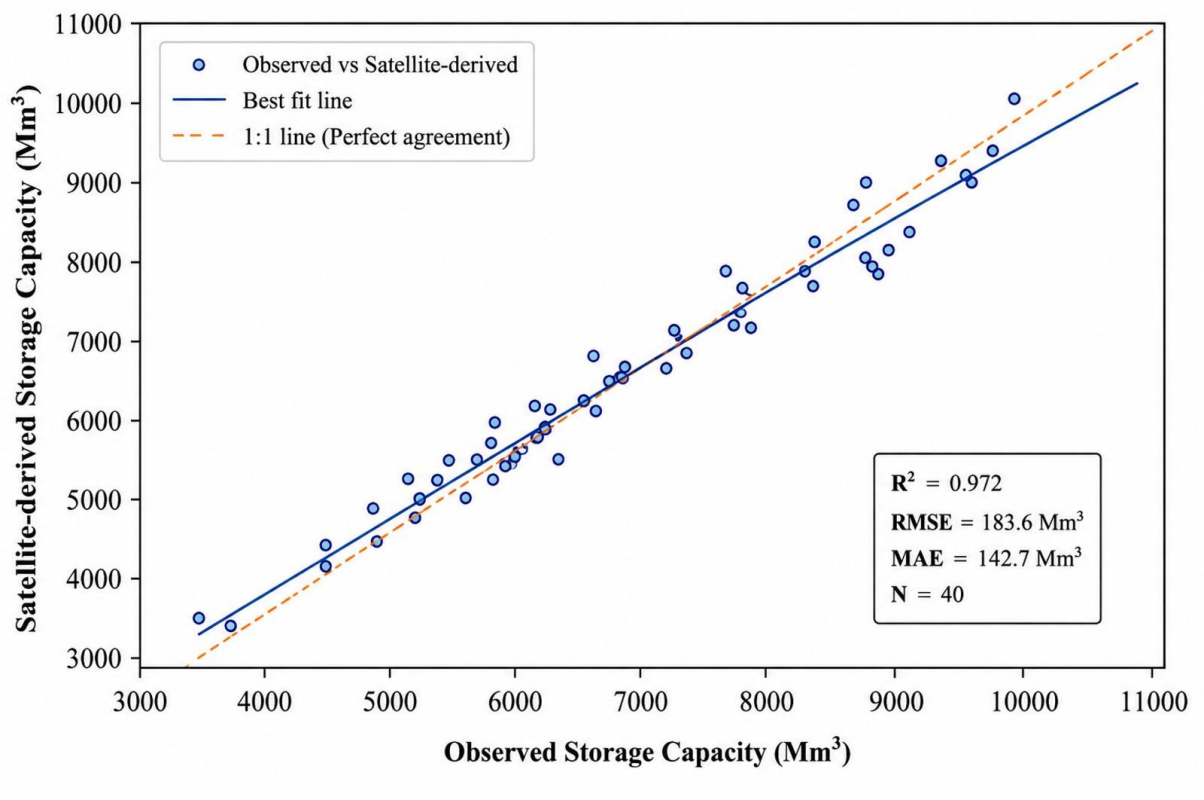


Figure-8: A comparison of storage capacity derived from satellite data and on-site observations.

4.3 The Assessment of Sedimentation

All reservoirs across the world experience sedimentation of varying degrees. It has drawn the attention of hydrologists and water resources mangers equally well. World Commission on Dams (2000) reported that reservoirs all around the world are filled up by sediments at a rate of approximately 1% every year. The annual storage loss of reservoir in terms of percentage for India is 0.46 (Choudhry et al. 2014). The depth of accumulated sediment in a reservoir for a known period can be measured by using echosounder and other electronic devices since the normal sounding operations provide erroneous results for large depths (Dutta,2016). However, the most convenient methods to determine the sedimentation of a reservoir are the direct

measurement by hydrographic survey and the indirect measurement using the inflow outflow records of a reservoir.

As in case of other reservoirs, in Nagarjuna Sagar reservoir too there has been sedimentation since its commissioning in the year 1968. The gross storage capacity derived from Landsat-TM/OLI&TIRS for the year 2001 works out to be 10,061.33Mm^3 as against original gross storage capacity of 11,472.00Mm^3 (URL)indicating thereby a loss in the storage capacity to the tune of 1,410.67Mm^3 during 31years (Table-7). Moreover, the water storage capacity has dropped further during subsequent years. In the year 2022 the gross storage capacity of the reservoir as derived from Sentinel SAR has been estimated at 9,373.52$Mm^{3.}$ Thus, there has been a loss in the gross storage capacity of the reservoir to the extent of 2,098.48Mm^3 during the period1968 to 2022 (54years) accounting for a loss of 18.29% in the original storage capacity of the reservoir. It works out to be an annual loss in the storage capacity to the extent of 0.339%, as against average annual storage loss of 0.46% for Indian reservoirs (Chaudhry et al. 2014).

In a study carried out over Ghataprabha reservoir located in Belgaum district, Karnataka, India, dual polarization (VV and VH) Sentinel-1 SAR data for the period 2016-2017 has been used for estimation of water spread area and storage capacity (Prasad et al.,2018). Results show a loss of 171.732 Mm^3 in storage capacity with respect to original value estimated in 1974 . The loss of storage capacity during a 43 years period works out to be around 4 Mm^3/year. Further , the estimated sedimentation rate is very high as compared to designed rate of siltation i.e. 0.58 Mm^3/year.

Table-7Temporal variations in gross storage capacity of the reservoir.

Original gross storage capacity (Mm^3) in 1968*	Gross storage capacity (Mm^3) in 2001	Gross storage capacity (Mm^3) in 2022
11,472.00	10061.33	9,373.52

* Source: India-WRIS (https://indiawris.gov.in/wiki/doku.php?id=nagarjunasagar-somasila_link) accessed on 09-08-2025.

5.Conclusions

Periodic assessment of reservoir capacity is important in water resources management as it helps in improving water resources management. The study has demonstrated the potential of orbital sensor multi-temporal data in monitoring water spread in a reservoir, which in conjunction with the information on reservoir's water level helps estimating the storage capacity of the reservoir. In the present study the information on water level was taken from *on-site* measurements which was used in conjunction with water spread area derived from remotely sensed data. Results show a drop in gross annual storage capacity of the reservoir to the tune of 0.339% during the period 1968 to 2022.The availability of cloud-free optical sensor data during monsoon season continues to remain a challenging task in tropical regions. Owing the potential of imaging the terrain in presence of clouds SAR data have been proved very effective in this endeavour. Furthermore, radar altimeters with proven potential for providing information on water level could also be used in conjunction with optical and SAR data in reservoir capacity estimation (Abileah. and Vignudelli, 2011). The interferometric Synthetic Aperture Radar (InSAR) data providing the precise information on water levels across the season may further improve the accuracy of the storage capacity of reservoirs. Further improvements in the storage capacity of reservoirs calls for refining algorithms to handle spatial resolution challenges and further improvements in the classification accuracy in diverse environmental conditions (Nikolić and Vladan , 2024). With regard to delineation of water pixels by thresholding of SAR backscattering values by graphical method Souza et al.(2022) suggest incorporating a bias correction step for achieving better results since this method leads to biased results leading to underestimation of water pixels

Acknowledgements

J. Venkatesh places on record his heartfelt sincere thanks to Dr. G. Chandra Sekhar, supervisor and Former Practice Head WIPRO, Hyderabad , and Prof. I. V. Muralikrishna, co-supervisor and former Director, R&D and Director Institute of Science and Technologies , Jawaharlal Nehru Technological University, (JNTU), Hyderabad, India for their able guidance. He is also indebted to Prof. G V Narasimha Reddy, Principal, University College of Engineering, Science and Technology, JNTU, Hyderabad for providing necessary facilities and evincing keen interest during the course of investigation. Our heartfelt thanks are also due to Dr P. Pranay, Research Scientist, ICRISAT, Patancheru, Dr. P. Sridhar, Guest Faculty and Sri. T Jaya Babu,

Technical Assistant, Centre for Spatial Information Technology ,JNTU, Hyderabad for their timely technical support.

Funding: No funding was received from any source for conducting this study.

References

Abileah ,R. and Vignudelli, S. 2011: A Completely Remote Sensing Approach To Monitoring Reservoirs Water Volume. *Fifteenth International Water Technology Conference, IWTC-15 2011, Alexandria, Egypt.*

Asthana, B. N., and Khare, D. ,2022. Reservoir sedimentation. In Recent advances in dam engineering (pp. 265–288). Springer. https://doi.org/10.1007/978-3-030-32278-6_12).

Basson, G. R.,2009. Management of siltation in existing and new reservoirs. General Report Q. 89. Proc. of the 23rd Congress of the Int. Commission on Large Dams CIGB ICOLD (vol. 2).

Central Water Commission, 2021.Sedimentation assessment of Nagarjuna Sagar reservoir, Andhra Pradesh & Telangana, through satellite remote sensing. Technical report, Central Water Commission, Government of India.

Chaudhry, M. A., Habib-ur-Rehman, M., Akhtar, N. A. and Hashmi, H. N. ,2014. Modeling sediment deposition and sediment flushing through reservoirs using 1-D numerical model. Arabian Journal for Science and Engineering, 39(2), 647–658.

Choudhary, S.S.and Ghosh,S.K, 2022.Surface water area extraction by using water indices and DFPS method applied to satellite data. Sensing and Imaging, Volume 23, Issue 1, article id.33.

Chen J., Peng Gong, Chunyang He, Ruiliang Pu, and Peijun Shi, 2003. Land-Use/Land-Cover Change Detection Using Improved Change-Vector Analysis. Photogrammetric Engineering & Remote Sensing Vol. 69, No. 4, April 2003, pp. 369–379.

Churchill, M.A..1948.. Discussion of "Analysis and Use of Reservoir Sedimentation Data", by L. C. Gottschalk. Proceedings of Federal Interagency Sedimentation Conference, Denver, pp. 139-140.

Codjia A.K.D., Komlavi Akpoti, Moctar Dembélé, Roland Yonaba, Tazen Fowe, Soumahila Sankande, Modeste G. Déo-Gratias Koissi, Sander J. Zwart,2025.Estimating water

levels in reservoirs using Sentinel-2 derived time series of surface water areas: A case study of 20 reservoirs in Burkina Faso, International Journal of Applied Earth Observation and Geoinformation, Volume 139,2025,104523,ISSN 1569-8432, https://doi.org/10.1016/j.jag.2025.104523.

Döll, P., Fiedler, K., and Zhang, J., 2009. Global-scale analysis of river flow alterations due to water withdrawals and reservoirs, Hydrology and Earth System Sciences, 13, 2413–2432, doi:10.5194/hess-13-2413-2009, 2009.

Dutta, S. 2016.Soil erosion, sediment yield and sedimentation of reservoir: a review. Model. Earth Syst. Environ. 2, 123 (2016). https://doi.org/10.1007/s40808-016-0182-y

Feyisa, G. L., Meilby, H., Fensholt, R., and Proud, S. R.,2014. Automated water extraction index: A new technique for surface water mapping using Landsat imagery. Remote Sensing of Environment, 140(0), 23–35. https://doi.org/10.1016/j.rse.2013.08.029.

Fisher, A., Flood, N., and Danaher, T.,2016. Comparing Landsat water index methods for automated water classification in eastern Australia. Remote Sensing of Environment, 175, 167–182. https://doi.org/10.1016/j.rse.2015.12.055.

Garg, V. and Jothiprakash, V., 2008. Trap efficiency estimation of a large reservoir. ISH Journal of Hydraulic Engineering. 14. 88-101. 10.1080/09715010.2008.10514907.

Gianinetto, M., Villa, P., and Lechi, G.,2006. Post-flood damage evaluation using Landsat TM and ETM plus data integrated with DEM. IEEE Transactions on Geoscience and Remote Sensing, 44(1), 236–243. https://doi.org/10.1109/tgrs.2005.859952.

Goel, M. K., and Jain, S. K.1996: Evaluation of reservoir sedimentation using multitemporal IRS-1A LISS II data. *Asian Pacific Remote Sensing and GIS Journal,* 8, pp 39-43.

Goel, M.K., Jain, S.K., and Agarwal, P.K.,2002. Assessment of sediment deposition rate in Bargi Reservoir using digital image processing. *Hydrological Sciences Journal*, 47(S), pp S81-S92.

Gourgouletis, N.; Bariamis, G.; Anagnostou, M.N.; Baltas, E., 2022. Estimating Reservoir Storage Variations by Combining Sentinel-2 and 3 Measurements in the Yliki Reservoir, Greece. *Remote Sensing*2022, 14, 1860. https://doi.org/10.3390/rs14081860 .

Guo, Z., Wu, L., Huang, Y., Guo, Z., Zhao, J., and Li, N., 2022. Water-Body Segmentation for SAR Images: Past, Current, and Future. *Remote Sensing*, *14*(7), 1752. https://doi.org/10.3390/rs14071752.

Hanasaki, N., Kanae, S., and Oki, T.,2006.A reservoir operation scheme for global river routing models, Journal of Hydrology, 327, 22 41, doi:10.1016/j.jhydrol.2005.11.011, 2006.

Hilgert, S. Klajdi S.& Stephan F., 2024. Review of methods of sediment detection in reservoirs, International Journal of Sediment Research, Volume 39, Issue 1,2024,Pages 28-43,ISSN 1001-6279, https://doi.org/10.1016/j.ijsrc.2023.12.004.

Huang, C., Chen, Y., Zhang, S., Li, L., Shi, K., and Liu, R., 2016. Surface water mapping from Suomi NPP-VIIRS imagery at 30 m resolution via blending with Landsat data. Remote Sensing, 8(8), 631.

Huang, C., Chen, Y., Zhang, S., and Wu, J. ,2018. Detecting, extracting, and monitoring surface water from space using optical sensors: A review. Reviews of Geophysics, 56, 333–360. https://doi.org/ 10.1029/2018RG000598

Jawak, S. , Kulkarni, K. and Luis, A. 2015. A Review on Extraction of Lakes from Remotely Sensed Optical Satellite Data with a Special Focus on Cryospheric Lakes. Advances in Remote Sensing, 4, 196-213. doi: 10.4236/ars.2015.43016.

Jeyakanthan, V.S and Sanjeevi. S.,2013. Capacity survey of Nagarjuna Sagar reservoir, India using Linear Mixture Model (LMM) approach. International Journal of Geomatics and Geosciences 4(1):186-194.

Ji, L., Zhang, L., and Wylie, B.K.,2009. Analysis of Dynamic Thresholds for the Normalized Difference Water Index. *Photogrammetric Engineering and Remote Sensing, 75*, 1307-1317.

Landmann, T., Schramm,M.,Huettich, C., and Dech, S. ,2013. MODIS-based change vector analysis for assessing wetland dynamics in Southern Africa. Remote Sensing Letters, 4(2), 104–113.

McFeeters, S.K. 1996: The Use of the Normalized Difference Water Index (NDWI) in the Delineation of Open Water Features. *International Journal of Remote Sensing*1996, 17, 1425–1432.

Merina, N. R., Sashikkumar, M., Rizvana, N., and Adlin, R.,2016. Sedimentation study in a reservoir using remote sensing technique. Applied Ecology and Environmental Research, 14(4), 296–304.

Morris, G.L., and Fan Jiahua.,1998. Reservoir sedimentation handbook, New York.

Nikolić, Ratko and Bošković, Vladan,2024. Assessment of surface water detection using Sentinel-1 SAR data: Case study Vojvodina province. Tehnika. 79. 523-530. 10.5937/tehnika2405523N.

Obialor, C. A., Okeke, O. C., Onunkwo, A. A., Fagorite, V. I., and Ehujuo, N. N.,2019. Reservoir sedimentation: Causes, effects and mitigation. International Journal of Advanced Academic Research, Sciences, Technology and Engineering.

Otsu,N.,1979.A threshold selection method from gray-level histograms. IEEE transactions on systems, man, and cybernetics, 9 (979), pp. 62-66.

Patra, K.C.,2001. Hydrology and Water Resources Engineering, *Narosa Publishing House New Delhi.*

Peng Dingzhi, Shenglian Guo., Pan Liu, Ting Liu., 2006, Reservoir Storage Curve Estimation Based on Remote Sensing Data. Journal of Hydrologic Engineering,11(2) https://doi.org/10.1061/(ASCE)1084-0699(2006)11:2(165).

Pham-Duc, B., Prigent, C., and Aires, F.,2017. Surface Water Monitoring within Cambodia and the Vietnamese Mekong Delta over a Year, with Sentinel-1 SAR Observations. *Water*, *9*(6), 366. https://doi.org/10.3390/w9060366

Piyoosh, A. and Ghosh, Sanjay,K.,2017. Semi-automatic mapping of anthropogenic impervious surfaces in an urban/suburban area using Landsat 8 satellite data. GIScience and Remote Sensing. 54. 10.1080/15481603.2017.1282414.

Codjia A.K.D., Komlavi Akpoti, Moctar Dembélé, Roland Yonaba, Tazen Fowe, Soumahila Sankande, Modeste G. Déo-Gratias Koissi, Sander J. Zwart,2025.Estimating water levels in reservoirs using Sentinel-2 derived time series of surface water areas: A case study of 20 reservoirs in Burkina Faso, International Journal of Applied Earth Observation and Geoinformation, Volume 139,2025,104523,ISSN 1569-8432, https://doi.org/10.1016/j.jag.2025.104523.

Prasad N.R., Vaibhav Garg and Praveen K. Thakur,2018. Role of SAR data in water body mapping and reservoir sedimentation Assessment ISPRS Annals of the Photogrammetry, Remote Sensing and Spatial Information Sciences, Volume IV-5, 2018.

Rathore, D.S., Choudhary, A. and Agarwal, P.K.,2006. Assessment of sedimentation in Harakud Reservoir using digital remote sensing technique. *Journal of the Indian Society of Remote Sensing,* 34, pp 344-383.

Rausch, D.H and Heinemann,H.G., 1968. Reservoir Sedimentation Survey Methods. Research Bulletin 939. University of Missouri, May 1968.

Rokni, K., Ahmad, A., Selamat, A., and Hazini, S.,2014. Water feature extraction and change detection using multitemporal Landsat imagery. Remote Sensing, 6(5), 4173–4189.

Sankey, J. B., Kreitler, J., Hawbaker, T. J., McVay, J. L., Miller, M. E., Mueller, E. R., et al., 2017. Climate, wildfire, and erosion ensemble foretells more sediment in western USA watersheds. Geophysical Research Letters, 44(17), 8884–8892. https://doi.org/10.1002/2017GL073979.

Schott, J.R., C. Salvaggio, and W.J. Volchok, 1988. Radiometric image normalization using pseudo-invariant features, *Remote Sensing of Environment*, 26:1–16.

Sheffield, J., Wood, E. F., Pan, M., Beck, H., Coccia, G., Serrat-Capdevila, A., and Verbist, K. , 2018. Satellite remote sensing for water resources management: Potential for supporting sustainable development in data-poor regions. Water Resources Research, 54, 9724–9758.

Shen, Y., Liu, D., Jiang, L., Nielsen, K., Yin, J., Liu, J., & Bauer-Gottwein, P. ,2022. High-resolution water level and storage variation datasets for 338 reservoirs in China during 2010–2021. *Earth System Science Data*, **14**(12), 5671–5694. https://doi.org/10.5194/essd-14-5671-2022.

Smith, L.C., and Pavelsky, T.M., 2009. Remote sensing of volumetric storage changes in lakes. *Earth Surface Process and Landforms*, 34, 1353 – 1358.

Souza, W.d.O.; Reis, L.G.d.M.; Ruiz-Armenteros, A.M.; Veleda, D.; Ribeiro Neto, A.; Fragoso Jr., C.R.; Cabral, J.J.d.S.P.; Montenegro, S.M.G.L. 2022.Analysis of Environmental and Atmospheric Influences in the Use of SAR and Optical Imagery from Sentinel-1,

Landsat-8, and Sentinel-2 in the Operational Monitoring of Reservoir Water Level. Remote Sens. 2022, 14, 2218.

Torres R, Snoeij P, Geudtner D, Bibby, D, Davidson M, Attema E, Potin P, Rommen B, Floury N, Brown M, Navas Traver I, Deghaye P, Duesmann B, Rosich B, Miranda N, Bruno C, L'Abbate M, Croci R, Pietropaolo A, Huchler M. & Rostan F.2012. GMES Sentinel-1 mission. Remote Sensing of Environment, 120, 9-24.

Vibulsresth., Srisangthong, D., Thisayakorn, K., Suwanwerakamtorn, R., Wongpam, S., Rodpram, C, Leelitharn, S. and Jiltanaon, W.,1988. The reservoir capacity of Ubolratana dam between 173 and 180 meters above mean sea level, Asian-Pacific Remote Sensing GIS Journal1(1):1-10.

Vishwakarma, Y., Tiwari, H. and Jaiswal, R., 2015. Assessment of reservoir sedimentation using remote sensing technique with GIS model—A review. International Journal of Engineering and Management Research (IJEMR), 5(3), 411–417.

Vörösmarty, C. J., Sharma, K. P., Fekete, B. M., Copeland, A. H., Holden, J., Marble, J., and Lough, J. A.,1997. The Storage and Aging of Continental Runoff in Large Reservoir Systems of the World, 85 Ambio, 26, 210–219, 1997.

Wang,Y.,2002. Mapping extent of floods: What we have learned and how we can do better. Natural Hazards Review, 3(2), 68–73. https://doi. org/10.1061/(ASCE)1527-6988(2002)3:2(68).

Wang, Y.,2004. Using Landsat 7 TM data acquired days after a flood event to delineate the maximum flood extent on a coastal floodplain. International Journal of Remote Sensing, 25(5), 959–974.

Wang, H.-W. and G. M. Kondolf ,2014. Upstream sediment-control dams: Five decades of experience in the rapidly-eroding Dahan River Basin, Taiwan, J. Am. Water Resour. Assoc., doi:10.1111/jawr.12141.

Wang, X. and Hongjie Xie. 2018. A Review on Applications of Remote Sensing and Geographic Information Systems (GIS) in Water Resources and Flood Risk Management" Water 10, no. 5: 608. https://doi.org/10.3390/w10050608

World Commission on Dams, 2000.Dams and Development - A New Framework For Decision-Making World Commission on Dams, London UK (2000)

Xu, H., 2006. Modification of normalised difference water index (NDWI) to enhance open water features in remotely sensed imagery, *International Journal of Remote Sensing*, 27:14, 3025-3033, DOI: 10.1080/01431160600589179.

Yao, F., Wang, C., Dong, D., Luo, J., Shen, Z., & Yang, K. (2015). High-Resolution Mapping of Urban Surface Water Using ZY-3 Multi-Spectral Imagery. *Remote Sensing*, *7*(9), 12336-12355. https://doi.org/10.3390/rs70912336.

Yoon, Y. and Beighley, E., 2015. Simulating streamflow on regulated rivers using characteristic reservoir storage patterns derived from synthetic remote sensing data, Hydrological Processes, 29, 2014–2026, doi:10.1002/hyp.10342, 2015.

URLs

URLa http://www.pecad.fas.usda.gov/cropexplorer/global_reservoir/

URLb http://www.legos.obs-mip.fr/soa/hydrologie/hydroweb Last accessed onAugust06,2026

URLc http://tethys.eaprs.cse.dmu. ac.uk/RiverLake/shared/main Last Accessed on August06,2026.

URLd https://dahiti.dgfi.tum.de Last Accessed on August06,2026.

.